ARMY RESEARCH LABORATORY

I. Trace Analysis of NO/NO_2 Mixtures by Laser Photofragmentation/ Fragment Photoionization Spectrometry at Visible Wavelengths

by R. C. Sausa
and J. B. Simeonsson

ARL-TR-1857 December 1998

The findings in this report are not to be construed as an official Department of the Army position unless so designated by other authorized documents.

Citation of manufacturer's or trade names does not constitute an official endorsement or approval of the use thereof.

Destroy this report when it is no longer needed. Do not return it to the originator.

Army Research Laboratory
Aberdeen Proving Ground, MD 21005-5066

ARL-TR-1857 **December 1998**

I. Trace Analysis of NO/NO_2 Mixtures by Laser Photofragmentation/Fragment Photoionization Spectrometry at Visible Wavelengths

R. C. Sausa
Weapons and Materials Research Directorate, ARL

J. B. Simeonsson
Department of Chemistry, University of Iowa

Abstract

Trace concentrations of NO and NO_2 molecules are differentiated spectrally using a visible dye laser and a simple flow cell with a pair of miniature electrodes for ion detection. NO is detected near 452 nm by (2+2) resonance-enhanced multiphoton ionization via its $A^2\Sigma^+ - X^2\Pi$ (0,0) transitions, while NO_2 is detected by laser photofragmentation with subsequent fragment NO ionization via the $A^2\Sigma^+ - X^2\Pi$ (0,0) and (1,1) transitions. Spectral differentiation is possible since the internal energy of the NO photofragment differs from that of "ambient" NO. Measurement of vibrationally excited NO via its $A^2\Sigma^+ - X^2\Pi$ (0,3) band is also demonstrated at 517 nm. Rotationally resolved spectra of NO and fragment NO are analyzed using a multiparameter computer program based on two-photon energy-level expressions and line strengths for $A^2\Sigma^+ - X^2\Pi$ transitions. Boltzmann analysis of the $P_{12} + O_{22}$ branch of the (0,0) band reveals that the rotational temperature of fragment NO is approximately 500 K compared to room temperature NO. Limits of detection (S/N = 3) of NO and NO_2 are in the 20–40-ppbv range at 449.2, 450.7, and 452.6 nm for a 10-s integration time. The limit of detection of NO_2 at 517.5 nm is 75 ppbv. The analytical utility of the technique for ambient air analysis is evaluated and discussed.

Acknowledgments

We thank Dr. A. Kotlar of the U.S. Army Research Laboratory (ARL) for his fitting routine and many helpful discussions. This work was supported by the ARL Director's Research Initiative and the Strategic Environmental Research Development Program (SERDP) on cleanup (Army-713-94 and Army-729-94).

INTENTIONALLY LEFT BLANK.

Table of Contents

INTENTIONALLY LEFT BLANK.

List of Figures

INTENTIONALLY LEFT BLANK.

List of Tables

INTENTIONALLY LEFT BLANK.

1. Introduction

The development and application of laser-based methods for detecting various nitrogen oxides continues to be an area of active interest [1–10]. Recently, we reported the development of a laser-based photofragmentation/photoionization (PF/PI) spectrometry technique that is useful for detecting parts-per-billion (ppb) levels of NO_2 and other nitrogen oxides in ambient air [4]. This technique is simple to implement since it (1) employs a single tunable laser source operating near 226 nm to photofragment the analyte molecule and also excite the characteristic NO photofragment via its $A^2\Sigma^+ - X^2\Pi$ (0,0) band; (2) requires only modest laser pulse energies, approximately 10 μJ; (3) employs a total (nonselective) ion detection approach that utilizes two miniature stainless steel plate electrodes; and (4) can perform measurements at relatively high pressures (50–760 Torr), minimizing the need for high vacuum.

The PF/PI method was previously demonstrated to have simultaneously high sensitivity and selectivity for several nitrogen oxide compounds using laser excitation a 226 nm [4]. However, as implemented, only the total NO content of a given sample was measured since the different contributors to the measured NO^+ signal were not resolved. The ability to differentiate between NO and NO_2 is often desirable. Thus, it is of interest to determine whether the PF/PI approach can be used to measure trace concentrations of NO_2 in the presence of NO by probing the internal energy distribution of "ambient" NO and fragment NO generated from the photolysis of NO_2. Furthermore, it is of interest to investigate the use of visible laser radiation in the PF/PI approach, as frequency doubling the laser radiation generally increases the cost and complexity of the laser system. The successful utilization of a visible laser source would greatly enhance the applicability of the PF/PI approach and make it accessible to a wide range of smaller pulsed laser systems.

In our previous PF/PI studies we employed (1+1) resonance-enhanced multiphoton ionization (REMPI) by accessing the NO $A^2\Sigma^+ - X^2\Pi$ (0,0) band near 226 nm. An alternative approach is to employ a (2+2) REMPI via the same band using laser excitation near 452 nm. Several groups have studied NO and NO_2 in this wavelength region [11–18]. Previous studies of the fragmentation and

photoionization dynamics of NO_2 in the 400–500-nm range have indicated the potential for spectrally resolving the ionization of NO and NO_2 [11]. Also, (2+2) REMPI has been used previously to profile parts-per-million levels of NO in a methane/air flame [12]. However, the analytical utility of a (2+2) REMPI approach has not been investigated for measurements of these species under ambient conditions.

In the present study, we investigate the analytical merits of laser fragmentation and/or ionization for trace NO and NO_2 detection and spectral discrimination using a single-dye laser operating near 452 or 517 nm. The detection of NO and fragment NO, generated from the photolysis of NO_2, is accomplished by a (2+2) REMPI via the NO $A^2\Sigma^+ - X^2\Pi$ (0,0), (1,1), and (0,3) bands. Discrimination is accomplished by probing the vibrational and rotational distribution of both ambient and fragment NO. The technique is demonstrated for laboratory air analysis.

2. Experimental

The experimental apparatus has been described previously [4]. An excimer-pumped dye laser system with second harmonic generator (Lumonics, HYPER EX-400, HYPER DYE-300, and HYPER TRAK-1000) provided up to 10-mJ pulses at 452 nm. Pulse energies of 10–15-ns duration (fuel width half maximum [fwhm]) were monitored between measurements using a joulemeter (Molectron Detector Inc., J4–05). The pulse energies for these studies were nominally 1 mJ/pulse.

The photolysis/ionization cell consisted of a six-arm stainless steel cross with internal arm diameters of 3.6 cm. Quartz windows mounted on opposing arms of the cell provided optical access to the center of the cell, where two stainless steel planar electrodes served as ion/electron detectors. The laboratory constructed electrodes were each approximately 1.5 cm^2 in area and separated by 0.63 cm. Electrical contact to the electrodes (used for biasing and signal collection) was accomplished with a vacuum feedthrough flange mounted on the third arm of the cell. Collection voltages ranged from 0 to 400 V. Quartz prisms directed the laser beam to a 50-mm diameter suprasil lens (150-mm focal length), which focused the beam in the center of the electrodes to

optimize ion/electron collection. The lens was placed external to the cell. The beam waist in the focal region was estimated to be 90 μm in diameter, resulting in a maximum intensity of 10^8 W/cm^2. An estimation of the effective volume probed by the laser is approximately 10^{-5} cm^3 (equal to 2-mm pathlength and 6-cm^2 × 10^{-5}-cm^2 focal area).

The signal from the detection electrodes was amplified with a current amplifier (Keithley 427, gain 10^5–10^7 V/A, time constant 0.01 ms) that was connected as close as possible to the collection electrodes in order to minimize radio-frequency pickup along the signal cable. The amplified signal was then sampled by a boxcar averager or viewed in real time on a 125-MHz digital oscilloscope (LeCroy 9400). The boxcar output was acquired by a personal computer for storage and subsequent data analysis. The analytical sensitivity determinations were performed at a laser repetition rate of 10 Hz, with 100-shot averaging using a 15-μs boxcar gate, while spectral recording was accomplished using 10-shot averaging with 0.005- or 0.001-nm/s scan rates.

Samples were prepared by serial dilution of standard gases (NO or NO_2 in N_2 or air) with pure buffer gases (zero air or N_2, 99.998%). All gases were obtained from Matheson, except for NO_2 in air (6.2 ppm), which was obtained from Scott-Marrin. Samples were flowed at approximately 500 cm^3/min through the photolysis cell to prevent buildup of photolysis products. The photolysis cell volume was estimated to be 350 cm^3.

3. Results/Discussion

3.1 Vibrational Analysis. The following equations represent the processes involved in NO and NO_2 detection and discrimination:

$$NO\ X^2\Pi\ (\upsilon'' = 0, J''_{low}) \xrightarrow[2(452\ nm)]{2h\nu} NO\ A^2\Sigma^+\ (\upsilon' = 0, J'_{low}) \xrightarrow[2(452\ nm)]{2h\nu} NO^+\ (X^1\Sigma^+) + e, \quad (1)$$

$$NO_2\ \tilde{X}^2A_1 \xrightarrow[2(452\ nm)]{2h\nu} NO_2\ \tilde{B}^2B_2 \xrightarrow{predissociation} NO\ X^2\Pi\ (\upsilon'' = 0,1, J''_{high}) + O(^1D), \quad (2)$$

and

$$NO\ X^2\Pi\ (\upsilon'' = 0,1, J''_{high}) \xrightarrow[2(452\ nm)]{2h\nu} NO\ A^2\Sigma^+\ (\upsilon' = 0,1, J'_{high}) \xrightarrow[2(452\ nm)]{2h\nu} NO^+\ (X^1\Sigma^+) + e. \quad (3)$$

Equation (1) represents the (2+2) REMPI of ambient NO at 452 nm via the $A^2\Sigma^+$ intermediate state. The ionization process is enhanced since the energy of the $A^2\Sigma^+ - X^2\Pi$ (0,0) transitions are resonant with the energy of two quanta of 452-nm photons. It should be noted that the ambient NO Boltzmann population distribution favors the $\upsilon'' = 0$ level of the ground electronic state. For a temperature of 298 K, $(\upsilon'' = 0/\upsilon'' = 1) \sim 10^4$. Equations (2) and (3) reveal the laser PF/FD approach for NO_2 detection. NO_2 is excited in the $\tilde{B}^2B_2$ electronic state by a two-photon process at 452 nm. Subsequently, NO_2 predissociates yielding vibrationally and rotationally excited NO and $O(^1D)$. Differentiation of NO and NO_2 is thus possible by interrogating the electronic ground-state vibrational and rotational distributions of both ambient and fragment NO. It should be noted that the processes represented by equations (2) and (3) are very fast and occur within the laser pulse duration, approximately 10–15 ns (fwhm).

Shown in Figure 1 (A and B) are (2+2) REMPI spectra in the 443–454-nm region of fragment NO generated from the photolysis of NO_2 and ambient NO, respectively. The features in Figure 1A correspond to mostly NO $A^2\Sigma^+ - X^2\Pi$ (0,0) and (1,1) transitions, while the features in Figure 1B correspond to NO $A^2\Sigma^+ - X^2\Pi$ (0,0) transitions. Morrison, Rockney, and Grant [11] also observed features due to NO $A^2\Sigma^+ - X^2\Pi$ (0,0) and (1,1) transitions in the two-photon collisionless dissociation of NO_2 over the region from 425–455 nm. The features shown in Figure 1A near 444 nm are due to (2,2) transitions of the NO photofragment and, to the best of our knowledge, have never been reported. As the threshold for two-photon NO_2 dissociation at 444 nm is approximately [19] 41,000 cm^{-1}, there is sufficient energy to leave the NO photofragment in the $\upsilon'' = 2$ energy level of the ground electronic state. By contrast, the two-photon dissociation of NO_2 at 450 nm, represented

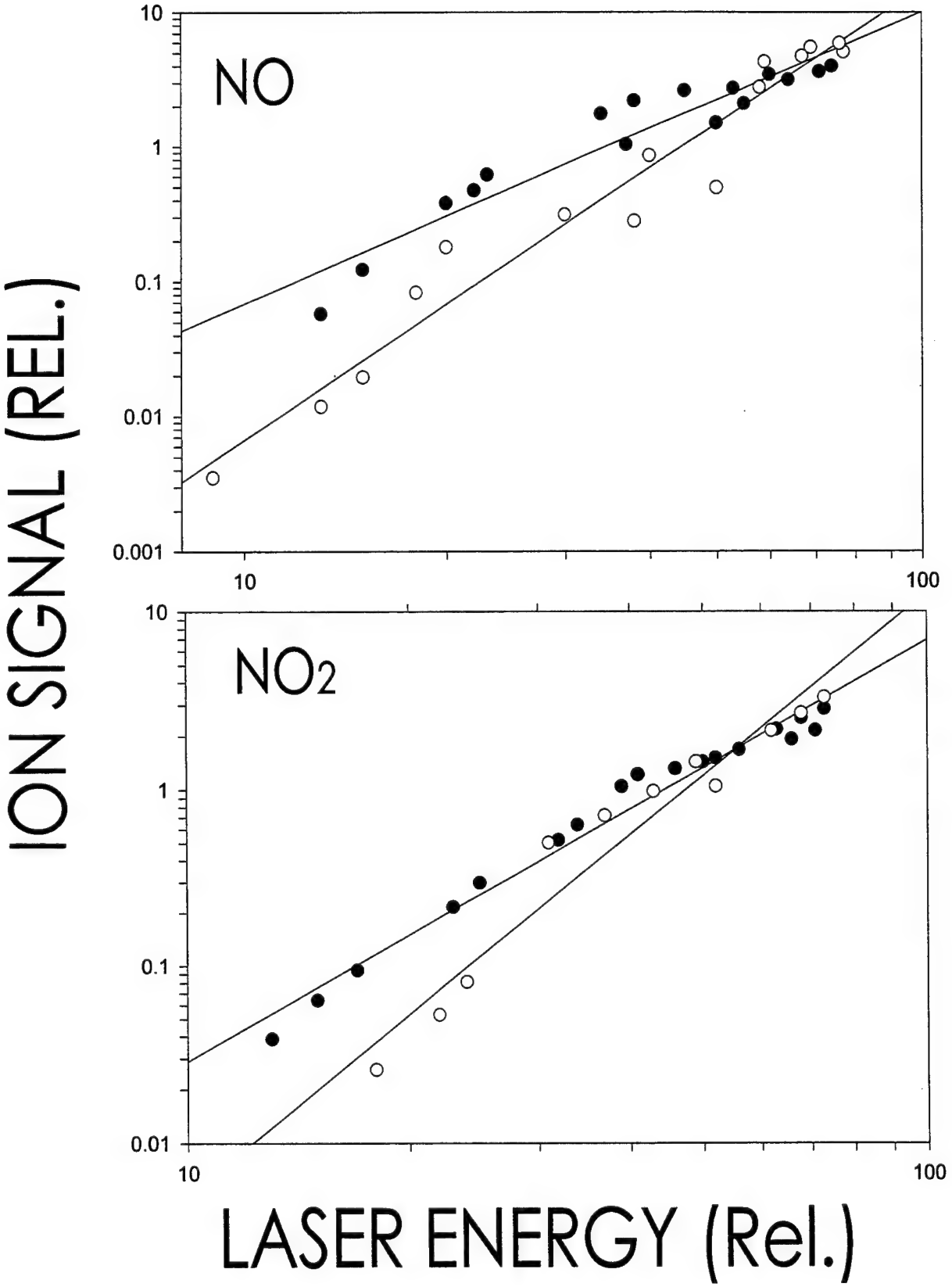

Figure 1. REMPI Spectra of ~6 ppm NO_2 in N_2 (A) and 0.1% NO in N_2 (B) in the Region of the $A^2\Sigma^+ - X^2\Pi$ A-X (1,1) and (0,0) Bands. The Spectra Are Not Corrected for Laser Energy Variation With Wavelength. The Total Pressure Was 100 Torr.

by equation (2), can only yield NO in the $\upsilon'' = 1$ state since it is the highest vibrational state that is energetically accessible. Morrison, Rockney, and Grant [11] did not observe any features due to NO $A^2\Sigma^+ - X^2\Pi$ (2,2) transitions, probably because their experiments were performed at low pressures (10^{-5} Torr) in a collision-free environment, in comparision to the high-pressure (100 Torr) collisional environment used in the present study.

The spectral feature near 449.2 nm in the NO_2 spectrum is attributed to the $O_{22} + P_{12}$ branch of the NO $A^2\Sigma^+ - X^2\Pi$ (1,1) band based on energy and similarity with the $O_{22} + P_{12}$ branch of the (0,0) band. This feature is populated as a result of the photofragmentation of NO_2, but is not observed for NO at ambient temperature. Figure 2 shows two high-resolution scans around 449 nm for NO and NO_2 and clearly demonstrates the absence of these features for ambient NO. This wavelength is a good candidate for monitoring NO_2 in the presence of NO, as ionization transitions in this region selectively indicate NO ionization that occurs as a result of NO_2 photofragmentation.

The spectral feature near 450.7 nm appears to be unusually strong when compared to other nearby lines. Although the vast majority of transitions in this spectral region occur by a (2+2) singly REMPI process where the second photon is resonant with NO $A^2\Sigma^+$ state, photoionization of NO near 450.7 nm is believed to occur by a double-resonance process, where both the second and third photons are resonant with excited states of NO. The overall mechanism is therefore described as a (2+1+1) REMPI process. The high intensity of this REMPI transition has been noted previously [14–18] and is attributed to a double resonance effect of the $J'' = 11\ 1/2$ line in the S_{21} branch, where the third photon is resonant with vibrational excited levels in the $B^2\Pi$, $K^2\Pi$, and $L^2\Pi$ states [15]. A study of the laser intensity dependence at this wavelength should indicate the presence of a double resonance by demonstrating a relatively lower order dependence on the laser intensity.

Shown in Figure 3 are plots of power dependence of the ion signal as a function of the incident laser intensity for NO and NO_2 at 450.7 and 452.6 nm ($J'' = 8\ 1/2$, $P_{11} + O_{21}$). The slopes of the data at 452.6 and 450.7 nm indicate the overall order of the photoionization processes. For NO, a (2+2) process (as at 452.6 nm) would be expected to show a dependence near 4; a (2+1+1) process (as at 450.7 nm) would also show a dependence of 4. However, under the relatively high laser intensities

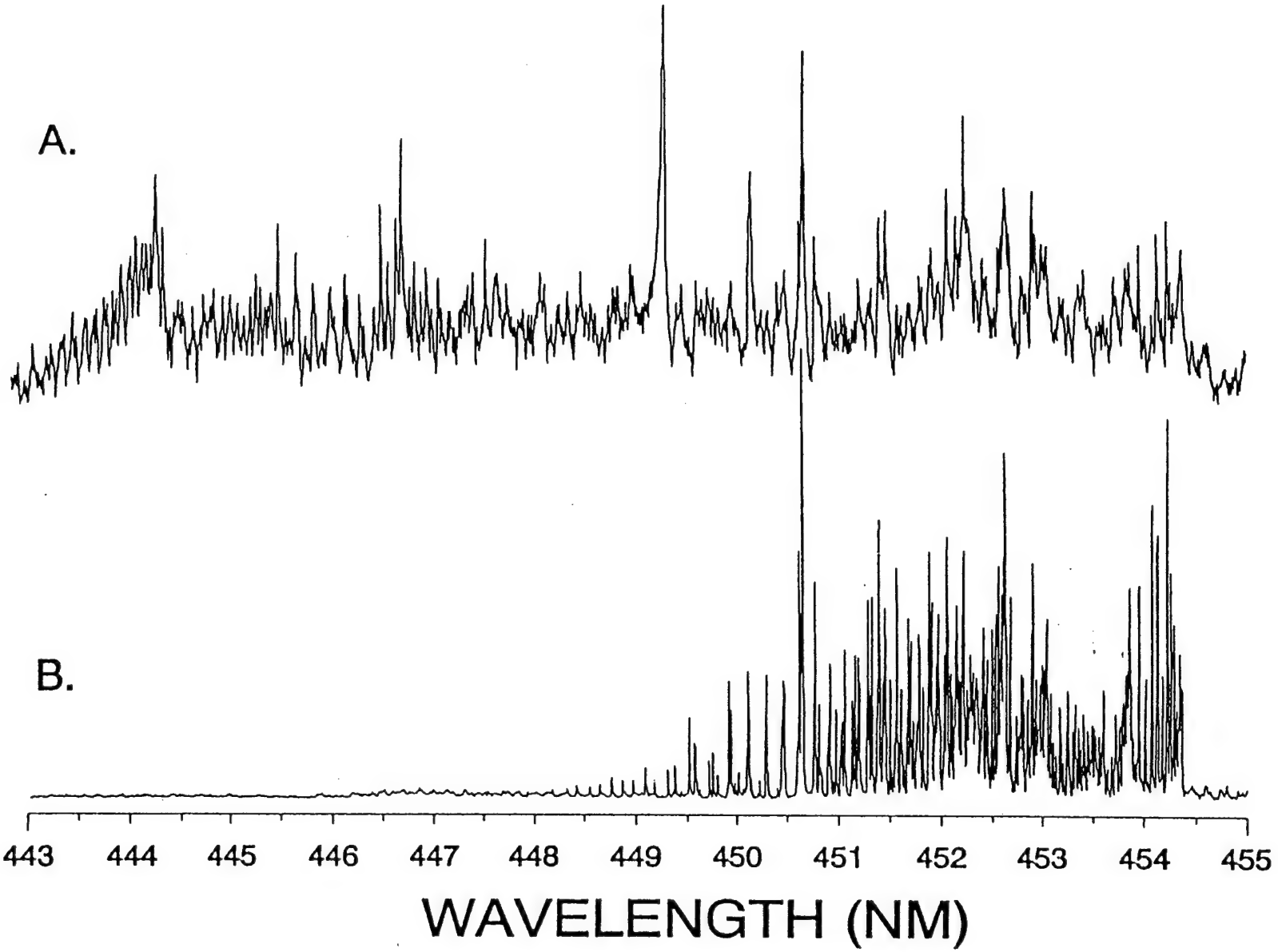

Figure 2. REMPI Spectra of Ambient NO (--) and Fragment NO From NO_2 (–) Near 449 nm Recorded at 100 Torr. The Features Correspond to O_{22} + P_{12} Branch Transistions of the NO $A^2\Sigma^+ - X^2\Pi$ (1,1) Band. Note the Absence of NO Ionization at the Branch Head.

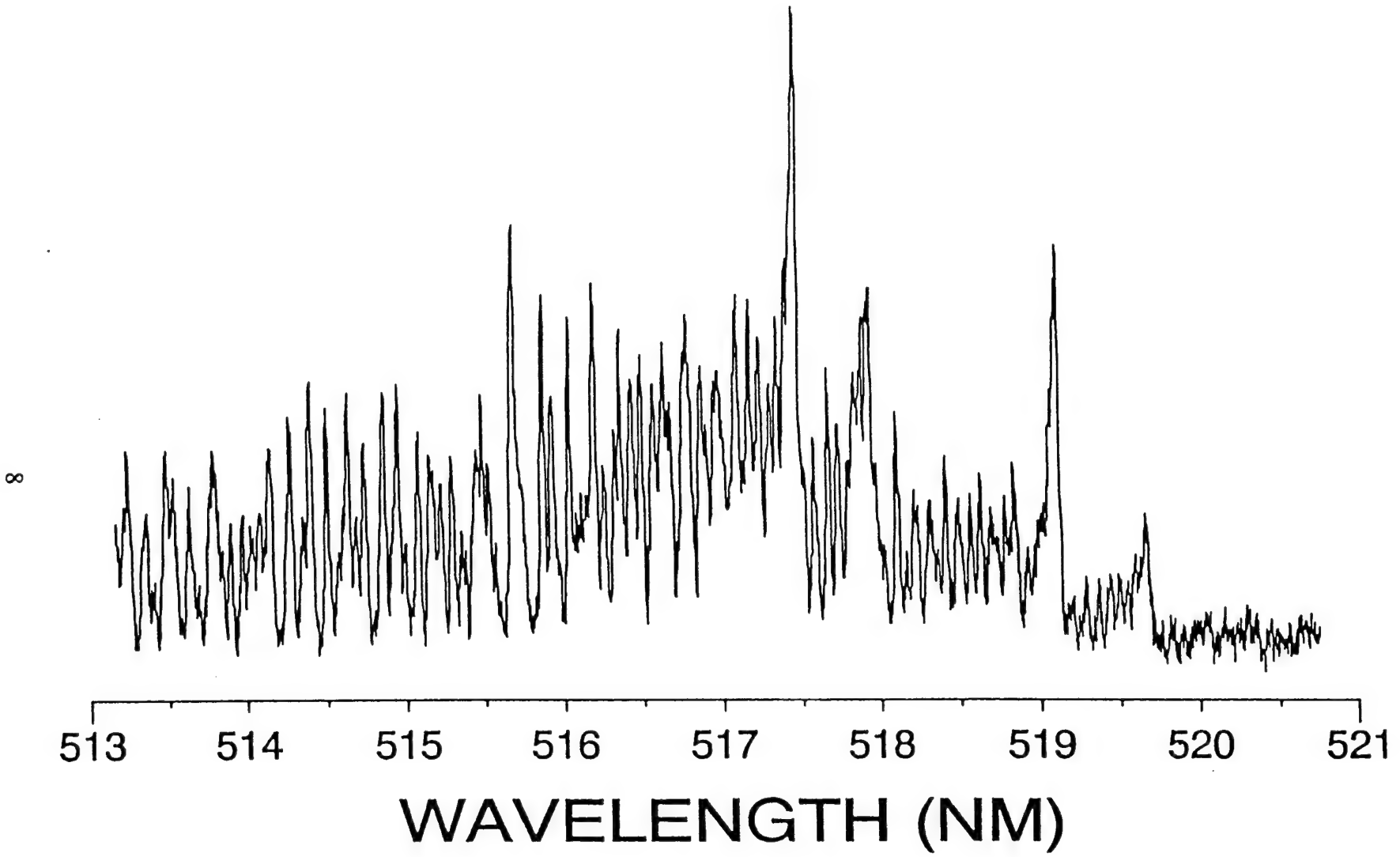

Figure 3. Plots of the NO REMPI Signal as a Function of the Laser Intensity at 450.7 nm (●) and 452.6 nm (○).

that are typically employed for multiphoton measurements, the third photon absorption is likely to be saturated or partially saturated. Under such conditions, a (2+1+1) process can reasonably be expected to show a dependence of 3 or less. The experimentally observed dependencies are 3.5 at 452.6 nm and 2.5 at 450.7 nm, respectively, each consistent with the proposed mechanisms and current experimental conditions. The results for NO_2 are nearly identical to those of NO at the two wavelengths, indicating that the multiphoton ionization process of fragment NO rather than NO_2 photofragmentation is rate limiting at the laser intensities used in this study.

In studies of the photofragmentation dynamics of NO_2, Morrison, Rockney, and Grant [11] observed significant fragmentation and ionization throughout the region from 430 to 520 nm. Above 500 nm, they observed several lines that were attributed to the direct photoionization of NO_2, including one at 511 nm, which was particularly strong. On the basis of the estimated ionization potential of NO_2, the threshold for four-photon ionization is 507.1 nm, and ionization at 511 nm would require at least five photons. Since NO does not exhibit significant multiphoton absorption in this spectral region, it appeared that it might be possible to selectively detect NO_2^+ ions at 511 nm. Unfortunately, our attempts at detecting this feature were unsuccessful. It should be noted, however, that our measurement conditions were significantly different from those of Morrison, Rockney, and Grant [11], whose ionization measurements of NO_2 were performed in a collisionless environment.

While investigating the region near 511 nm, we observed an unexpected series of lines. Shown in Figure 4 is a PF/REMPI spectrum of NO_2 extending from 513 to 521 nm. The band head formation and energy spacing of the branches bear a strong resemblance to those in Figure 1B. The rotational structure of the branches is also similar to that of Figure 1B, although the rotational lines do not reveal an enhancement due to double resonant multiphoton processes as in Figure 1B. The spectrum shown in Figure 4 corresponds to the $A^2\Sigma^+ - X^2\Pi$ (0,3) band of NO that results from the photofragmentation of NO_2. Following the two-photon photofragmentation of NO_2 at wavelengths between 513 and 520 nm, NO with υ'' up to 7 is likely to be produced by:

$$NO_2\ \tilde{X}^2A_1 \rightarrow NO\ X^2\Pi\ (\upsilon'' \leq 7) + O(^3P), \qquad (4)$$

since the threshold for this channel is approximately 25,000 cm^{-1}. The production of vibrationally excited NO by this channel continues with decreasing wavelength up to the point where the absorbed two-photon energy is sufficient to access the dissociation channel producing $NO(X^2\Pi) + O(^1D)$, represented by equation (2). Because of the lower energy carried away by the $O(^3P)$ atom fragment, the NO fragment's vibrational distribution for the channel represented by equation (4) is more energetic than the distribution for the channel represented by equation (2). Consequently, the detection of higher vibrational levels in the NO $X^2\Pi$ state is possible.

As there is minimal vibrational excitation of NO at ambient temperatures, the production and detection of highly vibrationally excited NO ($\upsilon'' \geq 3$) can theoretically be used to measure NO_2 while discriminating against NO. Although 521 nm is close to the direct four-photon multiphoton ionization wavelength for NO, direct multiphoton ionization of NO is unlikely, especially at the laser energies utilized (approximately 1 mJ). A spectral scan of NO from 513 to 521 nm produced negligible ion signals and did not show any of the $A^2\Sigma^+ - X^2\Pi$ (0,3) features seen in Figure 4.

3.2 Rotational Analysis. Discrimination of NO and NO_2 based on rotational temperature was also investigated. For a system described by a Boltzmann distribution, the ion signal in an optically thin region can be expressed as [20, 21]:

$$S_{ion} = F \int I_{\nu,o}(\nu_o)\, e^{(-h\nu/c)[N_T/Q(T)]\sum_j S_j P_j S_j g_j e^{-E_j}/kT}\, d\nu, \qquad (5)$$

where F is a scaling factor that includes system response, $I_{\nu,o}(\nu_o)$ is the laser frequency profile with intensity I centered at ν_o, h is Planck's constant, c is the speed of light, N_T is the total $NO(X^2\Pi)$ population, Q(T) is the partition function, S_j is the line strength for the jth transition, P_j is the Voigt transition lineshape, g_j is the degeneracy of the jth sublevel and E_j its energy, k is the Boltzmann constant; and T is the temperature. $I(\nu_o)$ was evaluated by numerical integration over ν. The limits of integration were chosen to include more than 99% of the laser profile.

The REMPI spectrum is generated by evaluating equation (5) for each (ν) value. The calculated spectrum is then fit to the observed spectrum using a multiparameter least-squares-fitting routine.

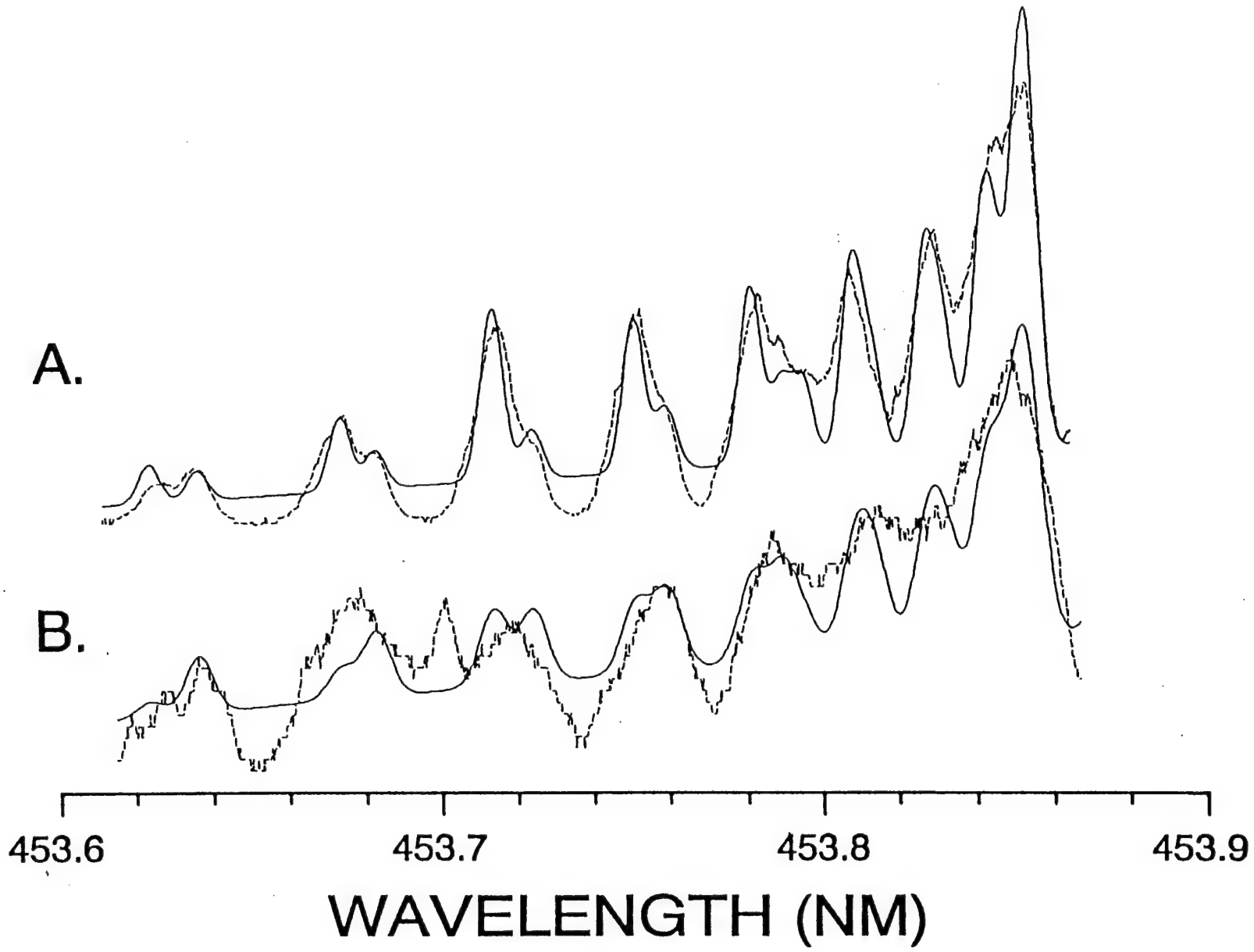

Figure 4. REMPI Spectrum of Fragment NO From NO_2 in the 513–521-nm Region Recorded at 100 Torr. The Features Correspond to Rotational Lines of the NO $A^2\Sigma^+ - X^2\Pi$ (0,3) Band.

Parameters include laser line shape, temperature, absolute and relative frequency values for the data, and parameters associated with experimental conditions. Doppler and collisional broadening are also accounted by the fitting routine. The standard deviation of each parameter, as statistically determined from the fit, is obtained from the computed variance/covariance matrix once convergence is achieved.

The $O_{22} + P_{12}$ branch of the NO $A^2\Sigma^+ - X^2\Pi$ (0,0) band was chosen for spectral analysis because it does not contain any (2+1+1) double resonance-enhanced rotational lines. These lines complicate the spectrum and make spectral analysis difficult since their transition probabilities are not known. The computer program utilized two-photon NO $A^2\Sigma^+ - X^2\Pi$ (0,0) transition probabilities obtained from a paper published by Halpern, Zacharias, and Wallenstein [22] and rotational energies generated using spectroscopic constants reported in Herzberg [23]. The line strengths associated with nonresonant continuum transitions from the $A^2\Sigma^+$ were assumed to be equal, similar as in (1+1) NO REMPI [24]. To test the program and verify our assumption, a REMPI spectrum of room temperature NO (0.1% in N_2) at 100 Torr was simulated using a Gaussian function for the laser line shape. The observed and calculated spectra are shown in Figure 5A. The best fit of the observed data yields a rotational temperature of 290 K ±10 K. Rotational analysis of fragment NO generated from the photolysis of NO_2 yields a temperature of 500 K ±100 K, suggesting that thermal equilibration has not been established at 100 Torr. By comparing simulation spectra with experimental spectra, Morrison and Grant [13] measured a temperature of 900 K ±100 K for nascent NO in a collisionless dissociation of NO_2 at 453 nm. Our value is consistent with the reported value since collisions help thermalize the nascent NO rotational distribution, thus lowering the temperature. For our experimental conditions, NO_2 experiences approximately 10 collisions with the buffer gas within the laser pulse duration. The differences in the rotational populations that are observed for ambient NO and fragment NO indicate the feasibility of spectroscopic differentiation of NO_2 from NO by the laser photofragmentation/fragment ionization approach.

3.3 Analytical Characterization. It is evident from the spectra that fragment NO generated from NO_2 exhibits prominent features that are absent in the ambient NO spectrum. These spectra suggest that the sources of detected NO can be resolved through spectral differences. From an inspection of the (2+2) REMPI spectra, several wavelengths have been identified as potentially

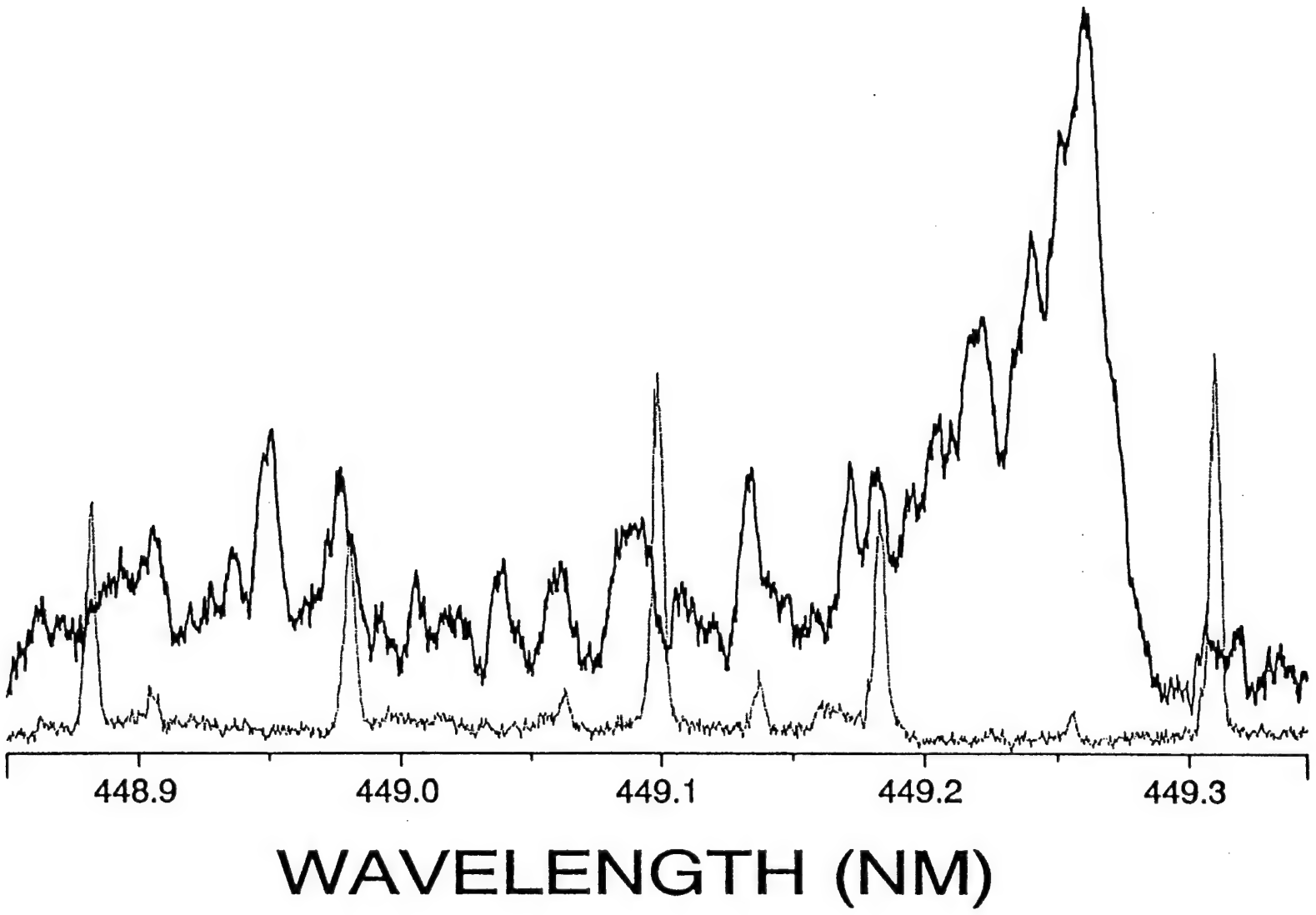

Figure 5. Observed (--) and Calculated (-) Spectra of the $O_{22} + P_{12}$ Branch Near 454 nm for 0.1% NO in N_2 (A) and Fragment NO Generated From the Photolysis of 6 ppm NO_2 in Air (B) at 100 Torr. The Simulations Are Best Fit of the Data and Yield Boltzmann Rotational Temperatures of 290 K ±10 K for Spectrum A and 500 K ±100 K for Spectrum B.

useful for quantifying NO_x (NO_x=NO+NO_2) and also for resolving the contributions of these two components. Shown in Table 1 is a compilation of the limits of detection (LOD) for NO and NO_2 in N_2 at 449.2, 450.7, 452.6, and 517.5 nm, and also for 226-nm excitation [4]. Similar results were obtained when air was used as the buffer gas. The LODs are defined as the concentration that yields a signal (at the indicated wavelength) equivalent to 3σ, where σ is the noise that is defined as the standard deviation of 16 independent measurements of the signal off resonance in zero air [4]. In terms of the LOD, the relative sensitivity is seen to be very similar at 449.2, 450.7, and 452.6 nm for NO_2. The LOD is somewhat higher at 517.5 nm, indicating a reduced sensitivity. Possible explanation for this observation include: (1) a relatively lower two-photon absorption of NO_2 at the 517.5 nm resulting in a relatively small population density in the $X^2\Pi$ ($\upsilon'' = 3$); (2) smaller multiphoton ionization cross sections of fragment NO at 517.5 nm; and (3) different channel for NO formation: more vibrational levels of the ground state manifold are accessible (up to $\upsilon'' = 7$) at 517.6 nm in comparison to the $\upsilon'' = 0$ and 1 levels, which can be accessed at 449.2, 450.7, or 452.6 nm.

Table 1. NO and NO_2 LODs at Various Wavelengths

Species	449.2 nm	450.7 nm	452.6 nm	517.5 nm	226.3 nm [4]
NO	n.d.	25	16	n.d.	1
NO_2	25	24	15	75	22

Notes: n.d. = not detected.
All concentrations are in parts per billion by volume (ppbv).

It is interesting to compare the performance of the PF/REMPI method when performed in the ultraviolet (UV) at 226 nm by a (1+1) REMPI approach and in the visible near 452 nm by a (2+2) REMPI approach. As seen in Table 1, the NO_2 LOD at 226 nm is nearly identical to that at 449.2, 450.7, and 452.6 nm. Despite this apparent similarity, the measured sensitivities and noises are significantly different in these two spectral regions. The normalized sensitivity for NO_2 on our experimental system is about 4 V/ppm at 226 nm [4], while at visible wavelengths the sensitivity ranges from 0.80 V/ppm at 449.2 and 450.7 nm to 1.3 V/ppm at 452.6 nm. Furthermore, the noise of the background, σ, is a factor 4 lower in the visible at 455 nm (0.007 V) than in the UV at 224 nm

(0.030 V), even despite using much higher laser intensities in the visible. The reduction in sensitivity that occurs at 452.6 nm, which is expected due to the lower multiphoton absorption cross section, is thus offset by a corresponding reduction in background noise. It is interesting to note that the background noise measured at 455 nm (when referred to the amplifier input) corresponds to as few as 400 electrons/laser pulse (or about 4 pA during the laser pulse) at the collection electrodes.

Relatively higher background noise in the UV is understandable because of the higher cross section for nonresonant multiphoton ionization, which is much more favorable for a two-photon process (in the UV) as opposed to a three-, four-, or even five-photon process (in the visible). For this reason, it is possible to use higher laser intensities in the visible without generating the same level of background. Relatively lower background contributions in the visible suggest that it is possible to increase the PF/REMPI sensitivity by increasing the laser intensity, perhaps up to the point of optical breakdown. It should also be possible to increase the sensitivity by increasing the focal length of the lens used to focus the laser in order to extend the laser's effective probe region.

Although there is a significant difference between the relative sensitivities of NO and NO_2 at 226 nm (roughly 1 order of magnitude), the relative sensitivities are nearly identical at 452.6 and 450.7 nm. This is presumably due to differences in the photofragmentation efficiencies in the two spectral regions, since the laser intensity in the visible is 2–3 orders of magnitude higher than in the UV. As the previous studies nominally employed 10-μJ pulse energies, high photofragmentation efficiencies could not be ensured for the precursors including NO_2. By ensuring a uniformly high photofragmentation efficiency, one can expect that the PF/REMPI approach will exhibit a more uniform sensitivity to NO and NO_2.

As discussed previously, there are two wavelengths (449.3 nm and 517.5 nm) at which NO_2 can be selectively detected (i.e., where ambient NO has negligible sensitivity). An effective measurement strategy for differentiating NO from NO_2 is to alternately measure the ion signal at 450.7 or 452.6 nm to determine the total NO and NO_2 content of the sample and then to measure the signal at 449.2 or 517.5 nm to selectively measure NO_2 signals that produce vibrationally excited NO photofragments. The difference in signals yields the concentration of ambient NO. Two independent measurements (different days) of laboratory room air were performed at 450.7, 452.6,

and 449.2 nm. The 449.2-nm wavelength was used for measuring the NO_2 concentration instead of the 517.5-nm wavelength because it was more sensitive and did not require changing the laser dye. With the use of sensitivities at 449.2, 450.7, and 452.6 nm shown in Table 1, $[NO_2]/[NO_x] \approx 3/5\ S_{449\,nm}/S_{453\,nm} \approx S_{449\,nm}/S_{451\,nm}$, where S is the ion signal. For the 449.2- and 452.6-nm wavelength pair, a $[NO_2]/[NO_x]$ value of ~1 with a NO_2 concentration of 200 ppbv was obtained for day 1, while a $[NO_2]/[NO_x]$ value of ~0.65 with a NO_2 concentration of 145 ppbv was obtained for day 2. Similar results were obtained using the 449.2- and 450.7-nm wavelength pair. The results show that there was a fair amount of NO_2 in the air with the NO_2 daily average concentration of 170 ppbv. While this level is high for indoor environments, the value is reasonable considering the amount of concentrated NO and NO_2 (>>parts per million by volume [ppmv] level) that was vented into the laboratory exhaust system, trace amounts of which leaked into the laboratory air during the course of our studies.

4. Summary/Conclusion

An investigation of the NO and NO_2 REMPI spectra reveals that these two species can be selectively monitored using visible radiation and a simple flow cell with total ion collection. Strong NO_2 signals due to vibrationally excited NO photofragments have been observed. The ion signals are due to NO $A^2\Sigma^+ - X^2\Pi$ (1,1) and (0,3) transitions near 452 and 517 nm, respectively. At these wavelengths, the sensitivity of room temperature NO is negligible. The presence of a doubly resonant feature at 450.7 nm, at which NO and NO_2 exhibit high sensitivity, has also been identified. The sensitivities for NO and NO_2 in the region 450 nm region are nearly identical with LODs in the 15–25-ppbv range and compare favorably with the sensitivity achieved previously for NO_2 at 226 nm. NO and NO_2 are also discriminated spectroscopically based on rotational temperature of ambient NO and fragment NO generated from the photolysis of NO_2. Rotational analysis of the $P_{12} + O_{22}$ branch of the NO A-X (0,0) band reveals that the rotational temperature of fragment NO is nearly 200 K higher than room temperature NO. The analytical utility of the approach using vibrational analysis has been demonstrated for ambient laboratory air. The approach allows the use of a simple apparatus and offers real-time and *in situ* monitoring capabilities. LODs in the low to sub-ppbv are projected with increased laser energy and improved system design.

5. References

1. Simeonsson, J. B., and R. C. Sausa. *Applied Spectroscopy.* To be published.

2. Lemire, G. W., J. B. Simeonsson, and R. C. Sausa. *Analytical Chemistry.* Vol. 65, p. 29, 1993.

3. Simeonsson, J. B., G. W. Lemire, and R. C. Sausa. *Applied Spectroscopy.* Vol. 47, p. 1907, 1993.

4. Simeonsson, J. B., G. W. Lemire, and R. C. Sausa. *Analytical Chemistry.* Vol. 66, p. 2722, 1994.

5. Marshall, A., A. Clark, R. M. Deas, C. Kosmidis, K. W. D. Ledingham, W. Peng, and R. P. Singhal. *Analyst.* Vol. 119, p. 1719, 1994.

6. Bradshaw, J. D., M. O. Rodgers, S. T. Sandholm, S. KeSheng, and D. D. Davis. *Journal of Geophysical Research.* Vol. 90, p. 12861, 1985.

7. Sandholm, S. T., J. D. Bradshaw, K. S. Dorris, M. O. Rodgers, and D. D. Davis. *Journal of Geophysical Research.* Vol. 95, p. 10155, 1990.

8. Papenbrock, Th., and F. Stuhl. *Journal of Atmospheric Chemistry.* Vol. 10, p. 451, 1990.

9. Papenbrock, Th., F. Stuhl, K. P. Müller, and J. Rudolph. *Journal of Atmospheric Chemistry.* Vol. 15, p. 369, 1992.

10. George, L. A., and R. J. O'Brien. *Journal of Atmospheric Chemistry.* Vol. 12, p. 195, 1991.

11. Morrison, R. J. S., B. H. Rockney, and E. R. Grant. *Journal of Chemical Physics.* Vol. 75, no. 6, p. 2643, 1981.

12. Rockney, B.H., T. A. Cool, and E. R. Grant. *Chemical Physics Letters.* Vol. 87, no. 2, p. 141, 1982.

13. Morrison, R. J. S., and E. R. Grant. *Journal of Chemical Physics.* Vol. 77, no. 12, p. 5994, 1982.

14. Kimman, J., P. Kruit, and M. J. van der Wiel. *Chemical Physics Letters.* Vol. 88, p. 576, 1982.

15. Esherick, P., and R. J. M. Anderson. *Chemical Physics Letters.* Vol. 70, p. 621, 1980.

16. White, M. G., W. A. Chupka, M. Seaver, A. Woodward, and S. D. Colson. *Journal of Chemical Physics.* Vol. 80, p. 678, 1984.

17. Miller, J. C., and R. N. Compton. *Journal of Chemical Physics.* Vol. 75, p. 22, 1981.

18. Miller, J. C., and R. N. Compton. *Chemical Physics Letters.* Vol. 93, p. 453, 1982.

19. Okabe, H. *Photochemistry of Small Molecules.* New York, NY: Wiley, 1978.

20. Anderson, W. B., L. J. Decker, and A. J. Kotlar. *Combustion and Flame.* Vol. 48, p. 163, 1982.

21. Vanderhoff, J. A., and A. J. Kotlar. *Proceedings of the 23rd Symposium (International) on Combustion.* The Combustion Institute, p. 1339, Pittsburgh, PA, 1990.

22. Halpern, J. B., H. Zacharias, and R. Wallenstein. *Journal of Molecular Spectroscopy.* Vol. 79, p. 1, 1980.

23. Herzberg, G. *Molecular Spectra and Molecular Structure I. Spectra of Diatomic Molecules.* Van Nostrand, Princeton, 1950.

24. Jacobs, D. C., R. J. Madix, and R. N. Zare. *Journal of Chemical Physics.* Vol. 85, p. 5469, 1986.

NO. OF COPIES ORGANIZATION

2 DEFENSE TECHNICAL INFORMATION CENTER
DTIC DDA
8725 JOHN J KINGMAN RD
STE 0944
FT BELVOIR VA 22060-6218

1 HQDA
DAMO FDQ
D SCHMIDT
400 ARMY PENTAGON
WASHINGTON DC 20310-0460

1 OSD
OUSD(A&T)/ODDDR&E(R)
R J TREW
THE PENTAGON
WASHINGTON DC 20301-7100

1 DPTY CG FOR RDE HQ
US ARMY MATERIEL CMD
AMCRD
MG CALDWELL
5001 EISENHOWER AVE
ALEXANDRIA VA 22333-0001

1 INST FOR ADVNCD TCHNLGY
THE UNIV OF TEXAS AT AUSTIN
PO BOX 202797
AUSTIN TX 78720-2797

1 DARPA
B KASPAR
3701 N FAIRFAX DR
ARLINGTON VA 22203-1714

1 NAVAL SURFACE WARFARE CTR
CODE B07 J PENNELLA
17320 DAHLGREN RD
BLDG 1470 RM 1101
DAHLGREN VA 22448-5100

1 US MILITARY ACADEMY
MATH SCI CTR OF EXCELLENCE
DEPT OF MATHEMATICAL SCI
MAJ M D PHILLIPS
THAYER HALL
WEST POINT NY 10996-1786

NO. OF COPIES ORGANIZATION

1 DIRECTOR
US ARMY RESEARCH LAB
AMSRL D
J W LYONS
2800 POWDER MILL RD
ADELPHI MD 20783-1145

1 DIRECTOR
US ARMY RESEARCH LAB
AMSRL DD
J J ROCCHIO
2800 POWDER MILL RD
ADELPHI MD 20783-1145

1 DIRECTOR
US ARMY RESEARCH LAB
AMSRL CS AS (RECORDS MGMT)
2800 POWDER MILL RD
ADELPHI MD 20783-1145

3 DIRECTOR
US ARMY RESEARCH LAB
AMSRL CI LL
2800 POWDER MILL RD
ADELPHI MD 20783-1145

ABERDEEN PROVING GROUND

4 DIR USARL
AMSRL CI LP (305)

NO. OF
COPIES ORGANIZATION

ABERDEEN PROVING GROUND

42 DIR, USARL
AMSRL-WM-B,
A.W. HORST
AMSRL-WM-BD,
B.E. FORCH
G.F. ADAMS
W.R. ANDERSON
R.A. BEYER
S.W. BUNTE
C.F. CHABALOWSKI
S. COLEMAN
A. COHEN
R. CUMPTON
R. DANIEL
D. DEVYNCK
R.A. FIFER
J.M. HEIMERL
B.E. HOMAN
A. JUHASZ
A.J. KOTLAR
R. KRANZE
E. LANCASTER
W.F. MCBRATNEY
K.L. MCNESBY
M. MCQUAID
N.E. MEAGHER
M.S. MILLER
A.W. MIZIOLEK
J.B. MORRIS
J.E. NEWBERRY
S.V. PAI
R.A. PESCE-RODRIGUEZ
J. RASIMAS
P. REEVES
B.M. RICE
P. SAEGAR
R.C. SAUSA (2 CP)
M.A. SCHROEDER
R. SCHWEITZER
L.D. SEGER
J.A. VANDERHOFF
D. VENIZELOS
A. WHREN
H.L. WILLIAMS

REPORT DOCUMENTATION PAGE

Form Approved
OMB No. 0704-0188

1. AGENCY USE ONLY *(Leave blank)*	2. REPORT DATE	3. REPORT TYPE AND DATES COVERED
	December 1998	Final, Sep 94–Oct 95

4. TITLE AND SUBTITLE
I. Trace Analysis of NO/NO_2 Mixtures by Laser Photofragmentation/Fragment Photoionization Spectrometry at Visible Wavelengths

5. FUNDING NUMBERS
1L161102AH43

6. AUTHOR(S)
R. C. Sausa and J. B. Simeonsson

7. PERFORMING ORGANIZATION NAME(S) AND ADDRESS(ES)
U.S. Army Research Laboratory
ATTN: AMSRL-WM-BD
Aberdeen Proving Ground, MD 21005-5066

8. PERFORMING ORGANIZATION REPORT NUMBER
ARL-TR-1857

9. SPONSORING/MONITORING AGENCY NAMES(S) AND ADDRESS(ES)

10.SPONSORING/MONITORING AGENCY REPORT NUMBER

11. SUPPLEMENTARY NOTES

12a. DISTRIBUTION/AVAILABILITY STATEMENT
Approved for public release; distribution is unlimited.

12b. DISTRIBUTION CODE

13. ABSTRACT *(Maximum 200 words)*

Trace concentrations of NO and NO_2 molecules are differentiated spectrally using a visible dye laser and a simple flow cell with a pair of miniature electrodes for ion detection. NO is detected near 452 nm by (2+2) resonance-enhanced multiphoton ionization via its $A^2\Sigma^+ - X^2\Pi$ (0,0) transitions, while NO_2 is detected by laser photofragmentation with subsequent fragment NO ionization via the $A^2\Sigma^+ - X^2\Pi$ (0,0) and (1,1) transitions. Spectral differentiation is possible since the internal energy of the NO photofragment differs from that of "ambient" NO. Measurement of vibrationally excited NO via its $A^2\Sigma^+ - X^2\Pi$ (0,3) band is also demonstrated at 517 nm. Rotationally resolved spectra of NO and fragment NO are analyzed using a multiparameter computer program based on two-photon energy-level expressions and line strengths for $A^2\Sigma^+ - X^2\Pi$ transistions. Boltzmann analysis of the $P_{12} + O_{22}$ branch of the (0,0) band reveals that the rotational temperature of fragment NO is approximately 500 K compared to room temperature NO. Limits of detection (S/N = 3) of NO and NO_2 are in the 20–40-ppbv range at 449.2, 450.7, and 452.6 nm for a 10-s integration time. The limit of detection of NO_2 at 517.5 nm is 75 ppbv. The analytical utility of the technique for ambient air analysis is evaluated and discussed.

14. SUBJECT TERMS
laser photofragmentation/fragment detection, NOX detection/discrimination, spectroscopy, trace analysis

15. NUMBER OF PAGES
26

16. PRICE CODE

17. SECURITY CLASSIFICATION OF REPORT	18. SECURITY CLASSIFICATION OF THIS PAGE	19. SECURITY CLASSIFICATION OF ABSTRACT	20. LIMITATION OF ABSTRACT
UNCLASSIFIED	UNCLASSIFIED	UNCLASSIFIED	UL

INTENTIONALLY LEFT BLANK.

USER EVALUATION SHEET/CHANGE OF ADDRESS

This Laboratory undertakes a continuing effort to improve the quality of the reports it publishes. Your comments/answers to the items/questions below will aid us in our efforts.

1. ARL Report Number/Author ARL-TR-1857 (Sausa) Date of Report December 1998\

2. Date Report Received _____

3. Does this report satisfy a need? (Comment on purpose, related project, or other area of interest for which the report will be used.) _____

4. Specifically, how is the report being used? (Information source, design data, procedure, source of ideas, etc.) _____

5. Has the information in this report led to any quantitative savings as far as man-hours or dollars saved, operating costs avoided, or efficiencies achieved, etc? If so, please elaborate. _____

6. General Comments. What do you think should be changed to improve future reports? (Indicate changes to organization, technical content, format, etc.) _____

CURRENT ADDRESS

Organization

Name E-mail Name

Street or P.O. Box No.

City, State, Zip Code

7. If indicating a Change of Address or Address Correction, please provide the Current or Correct address above and the Old or Incorrect address below.

OLD ADDRESS

Organization

Name

Street or P.O. Box No.

City, State, Zip Code

(Remove this sheet, fold as indicated, tape closed, and mail.)

(DO NOT STAPLE)